

Three Dimensional Architectures of Ultra-High Density Semiconducting Nanowires Deposited on Chip

Kevin M. Ryan,[†] Donats Erts,[‡] Hakan Olin,[§] Michael A. Morris,[†] and Justin D. Holmes^{*†}

Contribution from the Department of Chemistry, Materials Section and Supercritical Fluid Centre, University College Cork, Cork, Ireland, Institute of Chemical Physics, University of Latvia, Rainis Blvd, 19LV-1586 Riga, Latvia, and Physics and Engineering Physics, Chalmers University of Technology, SE-41296, Göteborg, Sweden.

Received February 5, 2003; E-mail: j.holmes@ucc.ie

Abstract: We report a “clean” and fast process, utilizing supercritical carbon dioxide, for producing ultrahigh densities, up to 10^{12} nanowires per square centimeter, of ordered germanium nanowires on silicon and quartz substrates. Uniform mesoporous thin films were employed as templates for the nucleation and growth of unidirectional nanowire arrays orientated almost perpendicular to a substrate surface. Additionally, these nanocomposite materials display room-temperature photoluminescence (PL), the energy of which is dependent on the diameter of the encased nanowires. The ability to synthesis ultrahigh-density arrays of semiconducting nanowires on-chip is a key step in future “bottom-up” fabrication of multilayered device architectures for nanoelectronic and optoelectronic devices.

Introduction

Many technologies, including electronics, separation science, and coatings will be enhanced by the ability to control the structure of materials on a nanometer-length scale. The ability to pack high densities of memory storage and processing circuitry into specific nanoscale arrays, and utilize the unique transport properties associated with these architectures, is expected to lead to future generations of computer processors with device sizes many times smaller and faster than current silicon based processors. However, both physical constraints and economics are expected to limit continued miniaturization of electronic and optical devices using current “top-down” lithography based methods.¹ Consequently, alternative nonlithographic methodologies for constructing the smallest mesoscopic features of an integrated circuit will soon be needed. One promising nonlithographic strategy is the use of solution phase chemistry to promote the self-assembly of materials from precursor “building blocks” into complex mesoscopic architectures.²

One-dimensional (1D) structures, such as nanowires and carbon nanotubes, have enormous potential as building blocks for nanoscale structures as they can function both as devices and as the wires that access them. Ångström-level size control, originally developed for nanocrystals, has already been applied to low-defect semiconductor nanowires. In particular, Holmes et al.³ have developed a supercritical fluid solution phase

technique for producing silicon nanowires with tunable crystal orientation and controllable optical properties. Cui et al.⁴ have also demonstrated that carrier type (electrons, n-type; holes, p-type) and carrier concentrations in single-crystal silicon nanowires can be controlled during growth using phosphorus and boron dopants. One inherent problem with these approaches however, is that nanowires are formed as entangled meshes. Considerable effort has been expended by Lieber and co-workers^{4,5} to manipulate a number of these nanowire meshes into useful configurations for nanoscale electronic devices. However, on a practical level, these flow methods are unlikely to facilitate the assembly of nanowires into high-density nanochip architectures, which are predicted to contain in excess of 1×10^{10} components per chip before the end of this decade.⁶ The production of high-density nanowire arrays up to 10^{11} per cm^2 , has previously been achieved through the electrodeposition of metal nanowires within anodic aluminum oxide (AAO) templates.⁷ Although AAO is a good templating matrix, forming an ordered array of nanoscale channels is difficult and the channel dimensions are too typically large to engineer nanowires that exhibit quantum confinement effects.⁸

Recently, we reported a supercritical fluid (SCF) inclusion technique for producing arrays of silicon and germanium nanowires, between 4.5 and 7.3 nm in diameter, within the pores of mesoporous silica “powders”.^{9,10} Such a comprehensive filling

[†] Department of Chemistry, Materials Section and Supercritical Fluid Centre, University College Cork.

[‡] Institute of Chemical Physics, University of Latvia.

[§] Physics and Engineering Physics, Chalmers University of Technology.

(1) Maydan, D. *Mater. Sci. Eng.* **2001**, *A302*, 1.

(2) Huck, W. T. S.; Tien, J.; Whitesides, G. M. *J. Am. Chem. Soc.* **1998**, *120*, 8267.

(3) Holmes, J. D.; Johnston, K. P.; Doty, R. C.; Korgel, B. A. *Science* **2000**, *287*, 1471.

(4) Cui, Y.; Lieber, C. M. *Science* **2001**, *291*, 851.

(5) Cui, Y.; Duan, X.; Hu, J.; Lieber, C. M. *J. Phys. Chem. B* **2000**, *104*.

(6) Moore, G. E. *Electronics* **1965**, *38*, 1.

(7) Thurm-Albrecht, T.; Schotter, J.; Kastle, G. A.; Emley, N.; Shibauchi, T.; Krusin-Elbaum, L.; Guarini, K.; Black, C. T.; Tuominen, M. T.; Russell, T. P. *Science* **2000**, *290*, 126.

(8) Wernick, S.; Pinner, R.; Sheasby, P. G. *Anodic Films on Aluminium*; Scully, J. C., Ed.; Academic Press: New York, 1983; Vol. 23, pp 205–209.

of the mesopores with semiconductor nanowires effectively formed the first three-dimensional array of nanowires insulated at a finite distance of separation. Discrete transitions observed in the UV-Visible absorption and photoluminescence emission (PL) spectra of the silicon nanowires constrained within the mesoporous silica matrixes suggested that they possess unusual optical properties that could be exploited in a number of applications.¹¹ However, even though mesoporous powders are ideally suited for many purposes for other uses, such as templates for nanowire devices and interconnects, these mesoporous solids need to be cast as mesoporous thin-films (MTFs). In this paper, we describe the combination of mesoporous thin-film science with SCF technology to produce ordered high density arrays of quantum-confined germanium nanowires that could be utilized in future optical and electronic devices. For example, semiconducting nanowires of silicon and germanium constrained within transparent MTFs could potentially be used in very high-resolution screen displays, a potential key component in the expansion of information based technologies.¹²

Experimental Section

Preparation of Aluminosilicate Mesoporous Thin-Films (Al-MTFs). Aluminosilicate mesoporous thin-films (Al-MTFs) were produced based on a modification of the method described by Yoldas et al.¹³ for producing nonporous films. Tetraethoxy silane (TEOS, 25 g), ethanol (13 mL) and HCl (2.5 mL, 0.12 M) were mixed together in the presence of a surfactant (6–7 g), i.e., poly(ethylene oxide) (PEO)–poly(propylene oxide) (PPO) triblock copolymer surfactants, P85 (PEO₂₆PPO₃₉PEO₂₆), and P123 (PEO₂₀PPO₆₉PEO₂₀) (Uniquema, Belgium) or Brij 35 (C₁₂EO₂₃) (Sigma-Aldrich, Ireland). The resultant solution was stirred at 310 K for 10 min, to prehydrolyze the silica precursor, and then cooled in an ice bath prior to the addition of aluminum tri-*sec*-butoxide (Al(Obu)₃, 1 g). Finally, H₂O (25 mL) was added to the mixture and the solution was allowed to condense for 20 h prior to film casting. Polished silicon wafers and quartz slides were ultrasonically cleaned in triply distilled water prior to spin coating of the sol (2000–4000 rpm) for 30 s. The cast films were dried at 373 K for 40 min to complete the condensation process and subsequently calcined at 723 K for 1 h to effect complete template removal. Any residual surfactant was removed by flowing a 5% ozone stream (Yanco Ozone Generator GE60/MF 5000) over the silica for 30 min. In this manuscript “calcined mesoporous silicas” refers to silicas that have been both heat treated at 723 K and ozonized.

Preparation of Germanium Nanowire Arrays within Al-MTFs. Germanium nanowires were grown within the pores of Al-MTFs by the degradation of diphenylgermane in supercritical CO₂. Ordered Al-MTFs deposited on silicon wafers were coated with diphenylgermane and placed in a 100 mL high-pressure cell under an inert atmosphere. The cell was attached via a three-way valve, to a stainless steel reservoir (~21 mL). A high-pressure pump (Isco Instruments, PA) was used to pump CO₂ through the reservoir in to the reaction cell. The cell was placed in a furnace and heated to 873 K and pressurized to 37.5 MPa simultaneously using a platinum resistance thermometer and temperature controller. The reaction proceeded at these conditions for 30 min. The high pressures and temperatures used in these experiments and the volatile nature of the chemicals could potentially lead to fire or

explosion. Suitable safety precautions should be taken into consideration including the use of a blast screen.

Film and Nanowire Characterization. ²⁹Si Magic angle spinning nuclear magnetic resonance (MAS–NMR) data was collected on a Chemamagnetics 300 MHz CMX-lite apparatus with typical spinning frequencies of 5 kHz and pulse delays of 60 s due to the slow relaxation of the Silicon nucleus. High resolution transmission electron microscopy (HRTEM) data were collected on a (JEOL2010F field emission TEM), courtesy of Intel Oregon, with EDX attachment. Typically films were thinned using a focused ion beam.

Photoluminescence (PL) emission experiments were performed using a deuterium continuous discharge source and a spark discharge source of 6 ns duration in a helium–hydrogen gas mixture. The MTFs were contained in a variable temperature helium cryostat (4–360 K) with a nitrogen screen to avoid contamination of the sample surface. An X-ray tube with a tungsten anti-cathode (15 mA, 40 kV) was used to study luminescence under ionising radiation. PL emission was analyzed by a grating monochromator and detected by a photomultiplier (FEU-106).

Powder X-ray diffraction (PXRD) data was collected on a PANalytical XPERT PRO MPD diffractometer. CuK α radiation from an anode run at 40 kV and 40 mA was used in all experiments. An incident soler slit of 0.02 rad was used resulting in a 240 mm incident beam radius. The diffractometer was equipped with a programmable divergence slit which was used at minimum (0.03 mm) for low angle (2θ : 0.5–5) measurements and at maximum (4 mm) for high angle (2θ : 10–70).

Results and Discussion

Unidirectionally ordered MTFs have previously been formed by slow epitaxial-like growth from dilute solutions¹⁴ or by using electrical or magnetic fields to direct ordering.¹⁵ Films formed using these methods however typically lack the mechanical and thermal stability necessary to survive the high temperature (800 K) and high pressure (40 MPa) required for SCF nanowire inclusion. In this work, aluminum containing MTFs (Al-MTFs), templated from neutral triblock copolymer surfactants were used. Aluminum incorporation into the silica matrix was used to promote the hydrothermal and mechanical stability of the films. However, the higher reactivity and ease of dimerization of aluminum compared to silicon can lead to alumina segregation and loss of long range order in Al-MTFs.¹³ In our preparations aluminum was added at a predetermined time after silicon alkoxide hydrolysis had begun. This prehydrolysis step prevents dimerization of the alumina and ultimately results in the formation of Al-MTFs suitable for SCF processing.

Figure 1 shows a ²⁹Si MAS–NMR study of the sol formation process using the triblock copolymer P123 as a surfactant template. The unhydrolyzed sol, Figure 1a(i), shows a strong peak due to tetraethoxy silane (TEOS) at –82.3 ppm. Hydrolysis of the TEOS, as shown in eq 1, results in upfield resonances due to the formation of hydroxylated silicon species (Figure 1a(ii))



Sustained hydrolysis (Figure 1a(iii)) results in downfield resonances (< –82.3 ppm) as the hydroxylated silicon species condense further forming Q₁ (Si(OSi)(OH)₃) and Q₂ (Si(OSi)₂–

- (9) Coleman, N. R. B.; Ryan, K. M.; Spalding, T. R.; Holmes, J. D.; Morris, M. A. *Chem. Phys. Lett.* **2001**, *343*, 1.
 (10) Coleman, N. R. B.; O'Sullivan, N.; Ryan, K. M.; Crowley, T. A.; Morris, M. A.; Spalding, T. R.; Steytler, D. C.; Holmes, J. D. *J. Am. Chem. Soc.* **2001**, *123*, 7010.
 (11) Lyons, D. M.; Ryan, K. M.; Morris, M. A.; Holmes, J. D. *Nano Lett.* **2002**, *2*, 811.
 (12) Alt, P. M. *Single-Crystal Silicon for High Resolution Displays*; Toronto, Canada, 1997; Vol. M19.
 (13) Yoldas, B. J. *Non-Cryst. Solids* **1984**, *63*, 150.

- (14) Yang, K.; Kuperman, A.; Coombs, N.; Mamiche-Afara, S.; Ozin, G. A. *Nature* **1996**, *379*, 703.
 (15) Tolbert, S. H.; Firouzi, A.; Stucky, G. D.; Chmelka, B. F. *Science* **1997**, *278*, 264–268.

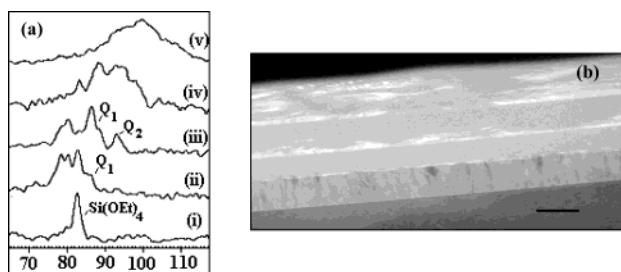


Figure 1. Characterization of directionally ordered Al-MTFs: (a) Stacked ^{29}Si MAS-NMR of silica and aluminosilicate hydrolysis, (b) TEM image of an ordered Al-MTF deposited on a silicon wafer (scale bar = 500 nm).

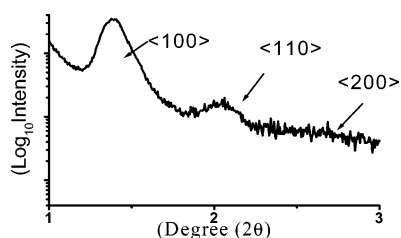
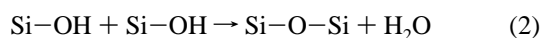
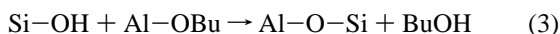


Figure 2. Low-angle PXRD profile from an Al-MTF prepared from the triblock copolymer P123.

(OH)₂ species according to eq 2



Significantly, aluminum incorporation, in the form of aluminum *sec*-butoxide, immediately prior to the onset of silicon self-condensation (eq 2) results in a highly homogeneous aluminosilicate matrix (eq 3). The aluminosilicate matrix showed MAS-NMR peaks at < -100 ppm (Figure 1a(iv)), with no evidence of alumina segregation



This prehydrolysis optimized functionalization of silica films with aluminum, in the presence of a surfactant template, results in transparent Al-MTFs with excellent substrate adherence, a hardness of up to 30 Gpa and thermal stability suitable to current microelectronic processing conditions.¹⁶ Figure 1b shows a TEM profile from an Al-MTF templated using the triblock copolymer P123 and prepared using the prehydrolysis technique. The Al-MTF is extremely uniform and well adhered to the substrate (film thickness, 400 nm). Effective control over film thickness can be facilitated, between 100 nm to 1 μm , by controlling the spinning rate during film casting.

Low angle PXRD analysis (Figure 2) of the Al-MTF shown in Figure 1b confirms that the film is highly ordered showing $\langle 100 \rangle$, $\langle 110 \rangle$, and $\langle 200 \rangle$ peaks characteristic of a hexagonal mesoporous solids.

The position of the intense $\langle 100 \rangle$ peak suggests a pore-center to pore-center repeat distance of 7.2 nm. Significantly, rotation of the thin film through the (ϕ) angle, clockwise in the xy plane, showed no significant loss in the $\langle 110 \rangle$ peak intensity. Ogawa et al.¹⁷ previously reported a loss in intensity of the $\langle 110 \rangle$ peak for silicate MTFs with pores aligned parallel to a substrate surface upon rotation through the (ϕ) angle. The intensity of the $\langle 110 \rangle$ diffraction peak for our Al-MTFs was found to change

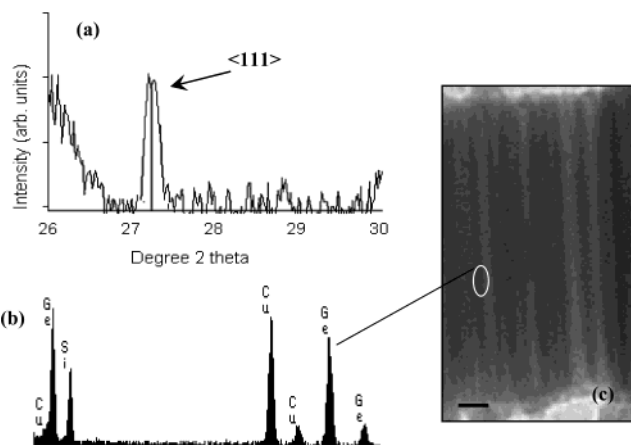


Figure 3. Ge nanowires within P85MTF: (a) high angle PXRD, (b) elemental analysis of wires in Figure 3c and (c) TEM image of wires constrained within mesoporous silica particle (scale bar = 25 nm).

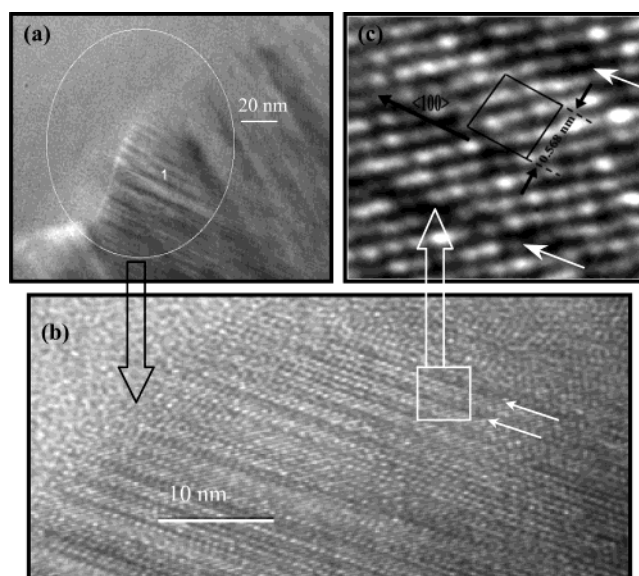


Figure 4. Germanium nanowires within Brij35 MTF: (a) High-resolution TEM image of germanium nanowires 2 nm in diameter constrained within the Al-MTF (scale bar = 20 nm), (b) magnified section showing atomic rows of single-crystal germanium ordered in the $\langle 100 \rangle$ direction (scale bar = 10 nm) and (c) magnified section of b showing unit cell of single-crystal germanium (scale bar = 0.568 nm).

significantly upon rotation of the sample through the (ψ) angle, in the yz plane. These results suggest that the mesopores within the P123 Al-MTF are ordered with the c -axis of the hexagonal phase almost perpendicular to the substrate surface. Similar results were also found with Al-MTFs templated from the surfactants P85 and Brij 35. However, the most compelling evidence for hexagonal pore growth perpendicular to the substrate surface is given in Figure 4a, which shows pore hosted nanowire growth almost perpendicular to the silicon wafer. Our results tie in well to those reported by Fukunaga et al.¹⁸ who have shown that rapid evaporation of solvent from triblock copolymer micelles in solution promotes the alignment of micelle aggregates perpendicular to a substrate surface. In our Al-MTF preparation, rapid solvent evaporation occurs upon spinning of the sol followed by aluminosilicate hydrolysis. To our knowl

(16) Mackenzie, J. D.; Ulrich, D. R. *Bk*; J. Wiley & Sons, Inc.: New York, 1988, 295–302.

(17) Ogawa, M. *J. Am. Chem. Soc.* **1994**, *116*, 7941–7942.

(18) Fukunaga, K.; Elbs, H.; Magerle, R.; Krausch, G. *Macromolecules* **2000**, *33*, 947.

edge, this is the first report of almost perpendicularly aligned Al-MTFs prepared by spin coating.

The degradation of germanium, from diphenylgermane, into the ordered channels of the Al-MTFs was undertaken using supercritical carbon dioxide as the fluid medium instead of supercritical hexane as previously used for silicon and germanium nanowire inclusion into mesoporous silica powders.^{9,10,19} CO₂ is a highly recyclable, cost-effective solvent and is less likely to contain potential dopant impurities present in organic solvents. Prior to Ge nanowire inclusion the Al-MTFs showed a type (IV) adsorption isotherm, typical for mesoporous solids. After nanowire inclusion, the surface area of the mesoporous silica films decreased typically from 700 to 600 m² g⁻¹ to 10–5 m² g⁻¹. Further evidence for nanowire inclusion was provided by high angle X-ray diffraction characterization of the germanium nanowires within the pores of the Al-MTFs (Figure 3a). Although, single crystal nanowires isolated within ordered mesoporous films are highly unlikely to be aligned at the correct angle for diffraction, rotation of the film through the phi angle (0–360°) resulted in a low intensity reflection from the ⟨111⟩ lattice plane of metallic germanium at $2\theta = 27.26$ reflecting a d spacing of 3.27 Å.

By careful selection of the surfactant template it is possible to control the pore size within Al-MTFs and hence the diameters of the nanowires formed within the pores. Direct visual evidence for nanowire formation within the mesoporous thin-films was provided by transmission electron microscopy (TEM). Figure 3b shows a TEM image of a particle cleaved from an Al-MTF templated from the triblock copolymer P85 filled with single-crystal germanium nanowires (P85Ge).

Parallel regions of high electron density are evident, approximately 4 nm in diameter, separated by a distance of approximately 2 nm. Elemental analysis of the dark parallel lines, by energy-dispersive X-ray analysis (EDXA), confirmed that nanowires of metallic germanium are hosted within an aluminosilicate matrix (Figure 3c). Both Si and Ge peaks are evident in the EDXA spectrum in addition to Cu from the microscopy grid. The length and aspect ratio of the wires suggest they are confined within an ordered matrix. It is highly unlikely that free-standing wires would form such directionally ordered arrays at a finite distance of separation without the templating matrix.

Figure 4a shows a high resolution TEM image of directionally ordered germanium nanowires constrained within a mesoporous silica thin-film templated from Brij35. Focused ion beam etching was used to reduce the film thickness to facilitate 200 KV TEM imaging. The constrained nanowires are approximately 2 nm in diameter, with a wall thickness of about 1 nm and have a packing density greater than 2×10^{12} nanowires per cm². Close analysis of the wires (Figure 4b) reveals the clear presence of atomic rows, which are not due to the amorphous aluminosilicate framework. A cubic cell geometry can be isolated (Figure 4c) with a unit cell lattice of 0.568 nm which agrees with that of crystalline germanium at 0.5657 nm in the literature. The wires appear to be orientated along the length of the mesopores in the ⟨100⟩ direction as shown in Figure 4c, which agrees with that previously reported for nanowires embedded within

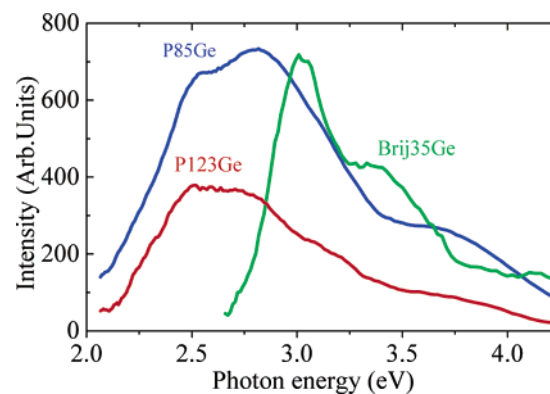


Figure 5. Ultraviolet PL emission spectra of germanium nanowires within mesoporous silica matrixes (excitation energy 4.89 eV).

mesoporous powders.⁹ The complexity of the cell can be attributed to beam penetration through multilayers of semiconducting nanowires. Close scrutiny of the atomic rows perpendicular to the wire direction reveals misalignment by up to 1/2 atom spacing as would be expected from multilevel wire arrays in a hexagonal lattice. In the hi-magnification image, the dark lines show high levels of contrast (indicated by the white arrows), which are most likely due to the mesoporous walls, which are totally random in structure (amorphous). These data agrees with high angle X-ray diffraction studies which do not pick up any crystallization of the Al-MTF matrix.

Our previous work on silicon nanowires constrained within tailored mesoporous silica powders showed that these nanocomposite materials display intense room-temperature UV and visible PL where the UV emission wavelength maximum is dependent on the diameter of the encased nanowires.¹¹ Figure 5 shows the normalized photoluminescence (PL) spectra for germanium nanowires constrained within Al-MTFs of 2, 4, and 5 nm pore sizes, templated from Brij 35 (Brij35Ge), P85 (P85Ge), and P123 (P123Ge) surfactants respectively on quartz substrates.

A shift in the PL emission maximum of the nanocomposite films to higher energies as the diameter of the germanium nanowires decreases is observed. PL is observed in the blue region, 2.64 eV, for 5 nm germanium nanowires encased in Al-MTFs which shifts to 2.75 and 3.01 eV for nanowires with diameters of 4 and 2 nm, respectively. The observed peak positions fit favorably to the energy of the lowest direct $1s_e \rightarrow 1s_h$ transition calculated from theoretical data of quantum confinement in nanocrystals and nanowires.^{20–23} A broad shoulder is also present, blue shifted with respect to the nanowire peak, for both P85Ge and Brij35Ge. This shift is possibly due to Si–O–Ge bonding at the pore wall-nanowire interface and has previously been attributed to germanium oxygen deficient centers or neutral oxygen monovacancies in germanium doped silica films.²⁴ The size dependent blue shifted PL strongly supports the hypothesis that the nanowires are constrained within the mesoporous silica matrix.

(20) Kayanuma, Y. *Phys. Rev. B* **1988**, *38*, 9797.

(21) Zacharias, M.; Fauchet, P. M. *Appl. Phys. Lett.* **1997**, *71*, 380.

(22) Kayanuma, Y. *Phys. Rev. B* **1988**, *38*, 9797.

(23) Brus, L. E. *J. Chem. Phys.* **1984**, *80*, 4403.

(24) Poulouios, D. P.; Spoonhower, J. P.; Bigelow, N. P. *J. Lumin.* **2003**, *101*, 23.

(19) Coleman, N. R. B.; Morris, M. A.; Spalding, T. R.; Holmes, J. D. *J. Am. Chem. Soc.* **2001**, *123*, 187.

Conclusions

In conclusion, ultrahigh density arrays of high purity germanium nanowires were synthesized perpendicularly orientated onto silicon and quartz substrates using supercritical carbon dioxide as an inclusion medium. The high-diffusivity of the fluid enables rapid transport of the germanium precursor into the mesopores of the silica thereby allowing swift nucleation and growth. Control over pore geometry allows the aspect ratio and optical properties of the included wires to be controlled with excellent precision. Ultimately, perpendicular arrays of 2 nm wires, insulated by 1 nm walls, allow for packing densities of up to 2×10^{12} wires per cm^2 , which will facilitate Moore's law extension for the next century.⁶ These nanowire arrays

potentially allow multilayered device formation using semiconducting nanowires as opposed to single level devices.^{4,5} Furthermore, the ability to control the optical properties of semiconductor wires in a transparent matrix at one thousandth the width of a human hair will allow for extremely high-resolution intelligent image displays with almost real resolution.

Acknowledgment. The authors acknowledge financial support from Enterprise Ireland, HEA Ireland and Intel (Ireland) Ltd. The authors would like to thank Juan Perez-Camacho, Anthony Hooper and Brian Davies for the HRTEM images. We also are grateful to Stephen Lipson for additional PL help.

JA0345064